A subclass of serum anti-ZnT8 antibodies directed to the surface of live pancreatic β-cells

Received for publication, September 29, 2017, and in revised form, October 22, 2017 Published, Papers in Press, November 28, 2017, DOI 10.1074/jbc.RA117.000195

Chengfeng Merriman[‡1], **Qiong Huang**[‡1,2], **Wei Gu**[§], **Liping Yu**[¶], **and Dax Fu**[‡3]

From the [‡]*Department of Physiology, Johns Hopkins School of Medicine, Baltimore, Maryland 21205, the* [§]*Section of Metabolic Disorders, Amgen Inc., Thousand Oaks, California 91320, and the* [¶]*Barbara Davis Center for Childhood Diabetes, University of Colorado Denver, Aurora, Colorado 80045*

Edited by Peter Cresswell

The islet-specific zinc transporter ZnT8 is a major self-antigen found in insulin granules of pancreatic β-cells. Frequent insulin secretion exposes ZnT8 to the cell surface, but the humoral antigenicity of the surface-displayed ZnT8 remains unknown. Here we show that a membrane-embedded human ZnT8 antigen triggered a vigorous immune response in *ZnT8* knock-out mice. Approximately 50% of serum immunoreactivities toward ZnT8 were mapped to its transmembrane domain that is accessible to extracellular ZnT8 antibody (ZnT8A). ZnT8A binding was detected on live rat insulinoma INS-1E cells, and the binding specificity was validated by a CRISPR/Cas9 mediated *ZnT8* knock-out. Applying established ZnT8A assays to purified serum antibodies from patients with type 1 diabetes, we detected human ZnT8A bound to live INS-1E cells, whereas a *ZnT8* knock-out specifically reduced the surface binding. Our results demonstrate that ZnT8 is a cell surface self-antigen, raising the possibility of a direct involvement in antibody-mediated β-cell dysfunction and cytotoxicity.

Zinc transport-8 (ZnT8)[4] is an islet-specific zinc transporter responsible for zinc enrichment in insulin secretory granules to enable insulin metalation and crystalline packaging (1). Peptides derived from ZnT8 have been identified as diabetogenic self-antigens both for $CD8^+$ and $CD4^+$ T-cells (2–6). Many targets of autoreactive T-cells are also humoral self-antigens recognized by serum autoantibodies, which are used as biomarkers for T-cell autoimmunity and type 1 diabetes (T1D) progression (7, 8). Serum autoantibodies directed against four major β-cell antigens: insulin (9), glutamic acid decarboxylase (10), IA-2 (insulinoma-associated protein 2) (11), and ZnT8 (12), allow autoimmunity to be confirmed in more than 96% of individuals newly diagnosed with T1D (13). Based on a partial ZnT8 antigen encompassing a cytosolic C-terminal domain (CTD, amino acids 275–369), serum ZnT8A was detected in 60–80% of sera from subjects with new onset T1D, including 26% ZnT8A-positive sera that were tested negative for other humoral T1D self-antigens (14, 15). At present, the anti-CTD ZnT8As are clinically used as a major biomarker in predicting T1D development in asymptomatic individuals at high risk.

Antibodies reactive to the cell surface of islet cells were observed in sera from children with T1D (16). A subclass of these antibodies was found to be β-cell–specific (17) and preferentially lytic for β-cells (18). These observations suggested a direct pathogenic role of surface-bound autoantibodies. However, the specificity of islet cell surface antibodies remains controversial (19, 20), and the molecular identity of the cell surface self-antigen is unclear. Previously, ZnT8 in insulin secretory granules was thought to be an intracellular self-antigen recognized by ZnT8A after T-cell–mediated β-cell destruction (12). We showed recently that the granular ZnT8 is trafficked to the surface membrane following insulin secretion (see Fig. 1*A*), thereby exposing its transmembrane domain (TMD, amino acids 60–266)) to serum ZnT8A recognition (21). By comparing the incidences of anti-CTD and anti-full-length ZnT8 (TMD+CTD) autoantibodies in 307 human sera from T1D diabetic and healthy control subjects (22), we detected a subclass of anti-TMD ZnT8A in the disease population. This finding raised the question as to whether serum anti-TMD ZnT8A in patients with T1D could recognize and react to ZnT8 on the surface of live pancreatic β-cells.

Here we present a full-length human ZnT8 antigen in reconstituted proteoliposomes (23). We first evaluated the antigenicity of the exposed extramembranous ZnT8 epitopes in mice based on humoral antibody responses to proteoliposome immunization. Full-length and partial ZnT8 antigens were used to determine the distribution of anti-TMD and anti-CTD ZnT8A in the polyclonal ZnT8A repertoire. We confirmed the conformation-specific ZnT8A binding to the full-length ZnT8 antigen, uncovered anti-ZnT8 immunoreactivity arising from TMD, and demonstrated specific anti-ZnT8 labeling of live rat insulinoma INS-1E cells (24) over a *ZnT8* KO background. Next, we implemented ZnT8A assays to detect ZnT8A in human sera from patients with T1D and healthy control subjects and quantify the ZnT8-specific immunoreactivity toward

This work was supported by National Institutes of Health Grant R01 GM065137. The authors declare that they have no conflicts of interest with the contents of this article. The content is solely the responsibility of the authors and does not necessarily represent the official views of the National Institutes of Health.

This article contains Figs. S1–S5.

[1] Both authors contributed equally to this work.

[2] Recipient of National Nature Science Foundation of China Grant GP 81673492.

[3] To whom correspondence should be addressed: Dept. of Physiology, Johns Hopkins School of Medicine, 725 North Wolfe St., Baltimore, MD 21205. Tel.: 443-287-4941; E-mail: dfu3@jhmi.edu.

[4] The abbreviations used are: ZnT8, zinc transporter-8; ZnT8A, ZnT8 antibody; CTD, C-terminal domain; T1D, type 1 diabetes; TMD, transmembrane domain; DOPC, 1,2-dioleoyl-*sn*-glycero-3-phosphocholine; DOPE, 1,2-dioleoyl-*sn*-glycero-3-phosphoethanolamine; DOPG, 1,2-Dioleoyl-*sn*-glycero-3-phosphoglycerol.

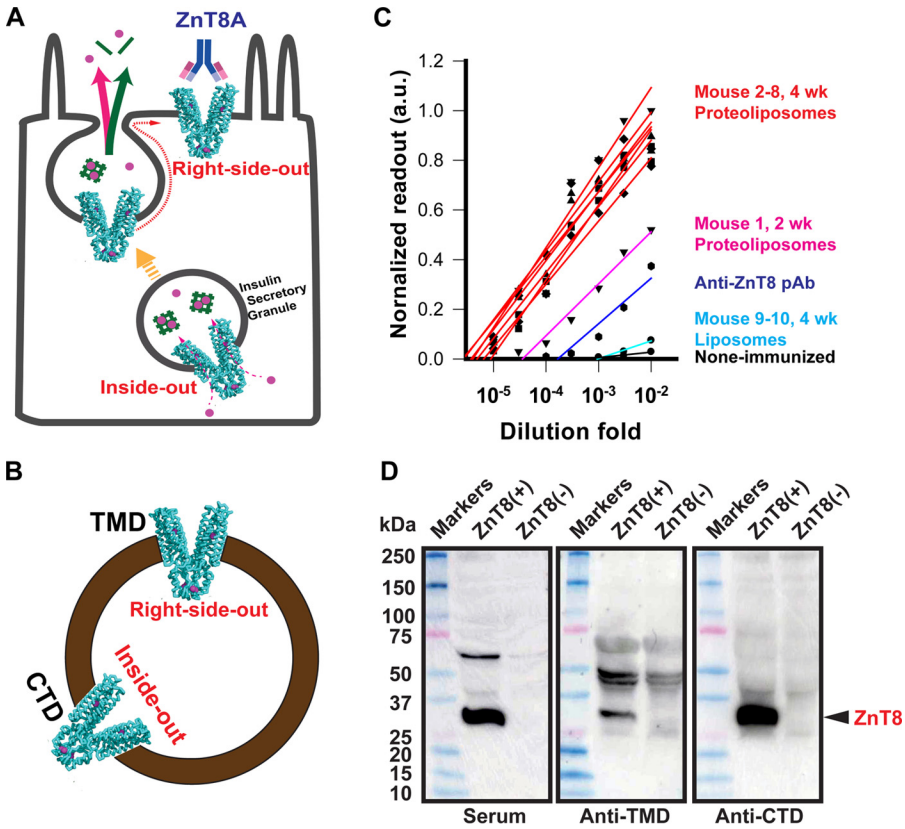

Figure 1. Humoral responses to human ZnT8 immunization in *ZnT8* KO mice. *A*, a schematic of surface display of granular ZnT8 (*cyan cartoon*) following insulin granule exocytosis in a pancreatic β-cell. The *green bars* and *magenta circles* represent insulin molecules and zinc ions, respectively. *B*, mixed transmembrane orientations of ZnT8 in a proteoliposome with both TMD and CTD exposed. *C*, titrations of serum anti-ZnT8 antibodies by proteoliposome-based ELISA using sera collected from seven mice with four weekly proteoliposome injections (*red lines*), one mouse with two weekly proteoliposome injections (*magenta line*), and two mice with four weekly liposome injections (*cyan lines*). Titrations with a commercial anti-ZnT8 pAb and non-immunized sera are shown as *blue* and *black lines*. *D*, immunoblotting of crude lysates of 293 cells with or without ZnT8 overexpression. ZnT8 (*black arrow*) in lysates was probed using a proteoliposome-immunized serum, anti-ZnT8 pAb (anti-TMD), or anti-ZnT8 mAb (anti-CTD) as indicated. Note, all proteoliposome-immunized sera showed a similar anti-ZnT8 immunoreactivity. Results from one representative serum are presented thereafter.

the surface of live INS-1E cells. Our results revealed a subclass of human ZnT8A directed to live β-cells. This finding provides the biochemical basis for exploring the potential pathogenic roles of surface-bound ZnT8A in antibody-mediated β-cell dysfunction and cytotoxicity in the development of T1D.

Results

Humoral anti-ZnT8 immune responses

The antigenicity of a full-length ZnT8 antigen was examined in mice. Recombinant human ZnT8 heterologously expressed in 293 cells was purified and reconstituted into proteoliposomes (23). Multiple copies of purified human ZnT8 proteins were inserted into a single proteoliposome with mixed transmembrane orientations, presenting both TMD and CTD on the extravesicular surface (Fig. 1*B*). The right-side-out ZnT8 exposed the extracellular surface of TMD, mimicking ZnT8 on the surface membrane of live β-cells (Fig. 1*A*). The inside-out ZnT8 adopted an opposite orientation, presenting CTD for immunization (Fig. 1*B*). Because of a high interspecies homology between human and mouse, the anti-ZnT8 immune response was interrogated in *ZnT8* KO mice to avoid the occurrence of central tolerance to human ZnT8 (25). The proteoliposome antigen was also immobilized to a 96-well microtiter plate to detect serum ZnT8A by ELISA. Assay calibration using a Proteintech anti-ZnT8 pAb demonstrated a linear titration curve in a logarithmic scale (Fig. 1*C*, *blue line*). Titrations of immunized mouse sera showed that intraperitoneal injection of proteoliposomes evoked a rapid and vigorous immune response. Two weeks after the initial proteoliposome injection, titrations of an proteoliposome-immunized serum yielded a titer of ~50,000, ~100-fold higher than the non-immunized control (Fig. 1*C*, *magenta line*). Two additional proteoliposome injections at weeks 3 and 4 led to additional ~10-fold boost of antibody titers in all seven animals (Fig. 1*C*, *red lines*). In sharp contrast, antibody titers for liposome immunization remained at the non-immunized background (Fig. 1*C*, *cyan* and *black lines*), indicating that the level of anti-lipid antibodies in sera was negligibly low. The serum anti-ZnT8 immunoreactivity was confirmed by immunoblotting of crude lysates from HEK293 cells. Comparing lysates from cells with and without ZnT8 overexpression, proteoliposome-immunized sera and two validated commercial anti-ZnT8 antibodies (anti-TMD and anti-CTD) detected a common protein band at a ~32-kDa position (Fig. 1*D*) ascribed to human ZnT8 previously (23). Because the membrane embedded region of TMD was not accessible to ZnT8A binding in proteoliposome-based ELISA detection, the observed ZnT8-specific antigenicity was attributed to extramembranous epitopes.

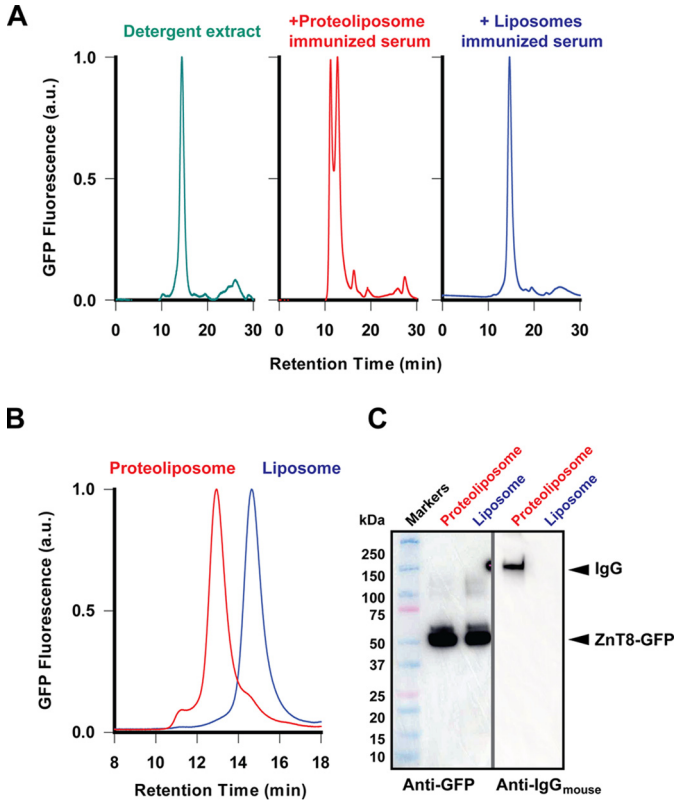

Figure 2. Binding of serum antibodies to ZnT8·GFP in its native conformation. *A*, analytical size exclusion HPLC revealed a single monodispersed ZnT8·GFP species in detergent micelles (*green trace*). Adding a proteoliposome-immunized serum to ZnT8·GFP formed ZnT8A-ZnT8·GFP complexes (*red trace*). Adding a liposome-immunized serum did not affect the ZnT8·GFP chromatogram profile (*blue trace*). *B*, formation of a 1:1 stoichiometric ZnT8A-ZnT8·GFP complex at a reduced serum-to-ZnT8·GFP ratio. The complex was only observed with proteoliposome-immunized sera as indicated. *C*, immunoblotting analysis of the proteoliposome or liposome peak fraction from *B*. ZnT8·GFP and ZnT8A were detected using an anti-GFP and anti-mouse IgG antibody as indicated.

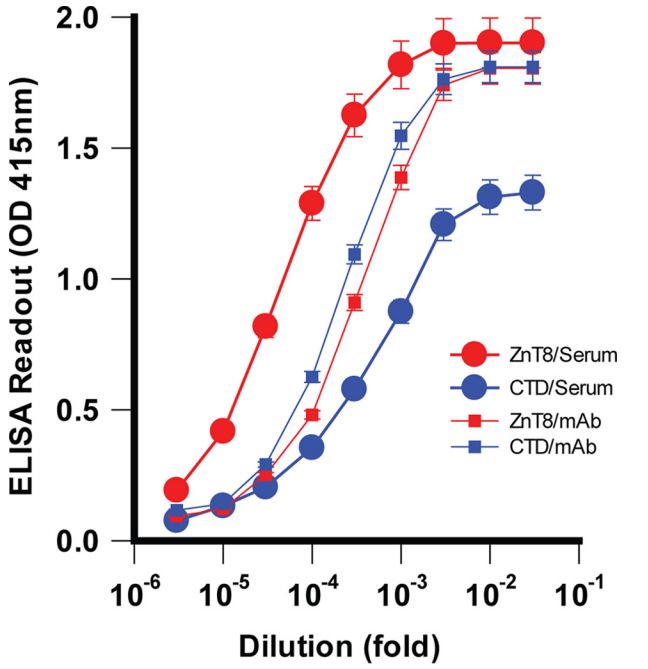

Figure 3. Distribution of ZnT8A epitopes in TMD and CTD. Purified ZnT8-His or CTD-His was immobilized for a comparative ELISA analysis. ZnT8 (TMD+CTD) and CTD responded approximately equally to titrations with an anti-CTD mAb (*small filled squares*) but exhibited marked difference in titrations with a proteoliposome-immunized serum (*large filled circles*). *Error bars* represent standard errors of three independent experiments.

Conformation-specific binding

The ZnT8A titers after four weekly proteoliposome injections were ~100-fold higher than the titer of the Proteintech anti-ZnT8 pAb directed to a linear epitope at the N terminus of TMD (Fig. 1*C*). The higher ZnT8A titers may reflect higher ZnT8A avidity involving the bindings of multiple immunodominant residues brought together by a proper folding of ZnT8 in a native state. To detect conformation-specific ZnT8A binding, we generated an INS-1E cell line that stably expressed human ZnT8 with a GFP appended to the C terminus. Detergent-solubilized ZnT8·GFP exhibited a major monodispersed peak by size-exclusion HPLC with fluorescence detection (Fig. 2*A*, *green line*). Adding a proteoliposome-immunized serum to ZnT8·GFP protein resulted in multiple peaks, indicating the formation of ZnT8A-ZnT8·GFP complexes in various multimeric states (Fig. 2*A*, *red line*). By comparison, the liposome-immunized serum did not alter the chromatogram profile of the unbound ZnT8·GFP peak (Fig. 2*A*, *blue line*). Reducing the serum-to-ZnT8·GFP ratio in the binding mixture reduced the multipeak profile to a single complex peak (Fig. 2*B*, *red line*), which was shifted leftward from the unbound ZnT8·GFP peak position (*blue line*) with an increase of 170 kDa, corresponding to the formation of an ZnT8A-ZnT8·GFP complex at a 1-to-1 binding stoichiometry as described previously (21). The formation of ZnT8A-ZnT8·GFP complex was confirmed by anti-GFP and anti-mouse-IgG immunoblotting (Fig. 2*C*). Both ZnT8·GFP and ZnT8A were detected in the peak fraction of higher molecular mass (Fig. 2*B*, *red line*), whereas ZnT8·GFP alone was detected in the peak fraction of lower molecular mass (Fig. 2*B*, *blue line*). The ability of proteoliposome-immunized sera to binding ZnT8 in a native conformation provided the experimental basis for immunodetection of native ZnT8 on the surface of live pancreatic β-cells.

Epitope mapping

The ZnT8 isoform 2 does not have a cytosolic N-terminal domain (26). A given ZnT8A epitope could be localized either in TMD or CTD. To characterize the distribution of ZnT8A epitopes between TMD and CTD, we performed a quantitative comparison of ZnT8A titrations against purified CTD and full-length ZnT8 (isoform 2). Both proteins contained an identical C-terminal His tag for immobilization to nickel-coated plates. Titrations with an Amgen anti-ZnT8 mAb directed to a C-terminal peptide epitope (Fig. S1) showed near superimposable titrations for immobilized CTD and ZnT8 (Fig. 3), indicating that both antigens responded approximately equally to ELISA detection of a common C-terminal epitope. When titrated with proteoliposome-immunized sera, however, the anti-ZnT8 titration curve was shifted leftward relative to the anti-CTD curve. The overall CTD/ZnT8 ratio calculated from all ELISA readouts in the titration curves was 0.46 ± 0.06 (n = 9), suggesting that ~50% of ZnT8A were directed to TMD, which could be accessible to ZnT8A binding on the surface of live β-cells as depicted in Fig. 1*A*.

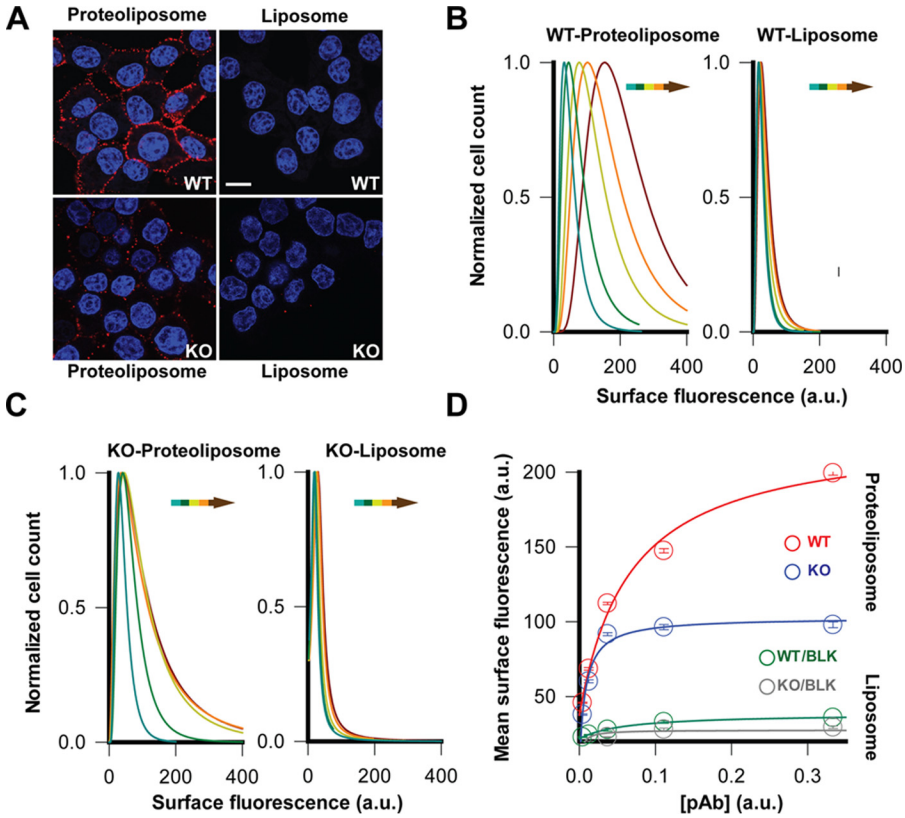

Figure 4. ZnT8-specific surface labeling of live INS-1E cells. *A*, representative confocal images of immunofluorescence staining of WT or *ZnT8* KO cells using a proteoliposome- or liposome-immunized serum as indicated. *Scale bar*, 20 μm. *B*, histograms of surface immunofluorescence intensities measured in >10,000 WT INS-1E cells that were stained by a proteoliposome- and liposome-immunized serum as indicated. The *solid lines* are least square fits to a Lorentzian distribution. *Arrows* indicate serum titrations with increasing concentrations. *C*, identical experiments in *B* except that *ZnT8* KO INS-1E cells were used. *D*, saturation of surface immunofluorescence staining with increasing serum concentrations. The concentration-intensity relationships were plotted using flow cytometry data in *B* and *C* (mean intensity ± S.E.). The *solid lines* are hyperbolic fits of concentration-dependent surface staining with a proteoliposome- or liposome-immunized serum as indicated.

Specific anti-ZnT8 labeling to the cell surface

To visualize ZnT8A binding on the surface of live cells, we exposed live INS-1E cells to proteoliposome-immunized mouse sera followed by anti-mouse IgG immunofluorescence staining at 4 °C. Confocal microscope imaging of INS-1E cells revealed a strong surface staining (Fig. 4*A*). By comparison, staining live INS-1E cells with a liposome-immunized mouse serum did not yield a detectable cell surface signal (Fig. 4*A*). We further evaluated ZnT8 specificity by comparing surface staining of WT and *ZnT8* KO INS-1E cells generated by CRISPR/CAS9-mediated gene deletion (27). Anti-ZnT8 immunoblotting of *ZnT8* KO cells confirmed the loss of ZnT8 expression (Fig. S2), and live-cell staining with a zinc indicator Zinpry-1 showed a 37% reduction of intracellular zinc fluorescence in *ZnT8* KO cells (Fig. S3). Concomitantly, staining *ZnT8* KO cells with proteoliposome-immunized sera revealed a significant reduction of surface immunofluorescence (Fig. 4*A*). The residual non-ZnT8 signals were apparently related to ZnT8 immunization because liposome-immunized sera stained neither WT nor KO cells (Fig. 4*A*). Thus, the immunofluorescence difference between WT and KO cells reflected ZnT8-specific labeling. The WT and KO difference was quantitatively evaluated over 10,000 live cells by flow cytometry (Fig. S4). The immunofluorescence of individual cells was recorded to construct an intensity distribution histogram, which was least squares–fitted to a Lorentzian distribution to calculate the mean intensity and standard error (Fig. 4, *B* and *C*). Staining live cells with proteoliposome-immunized sera progressively shifted the histogram rightward with an increasing serum concentration for WT cells (Fig. 4*B*) and to a lesser degree for KO cells (Fig. 4*C*). The surface immunofluorescence intensity approached saturation at higher serum concentrations where the WT-staining was 2.2-fold higher than the KO-staining with a proteoliposome-immunized serum (Fig. 4*D*). In contrast, no significant WT-KO difference was observed for surface staining with liposome-immunized sera at background levels (Fig. 4*D*). Taken together, the WT-KO difference obtained from cell population-based flow cytometry analysis gave a reliable measure of ZnT8-specific immunoreactivity toward the surface of live β-cells.

Immunoreactivity of human T1D sera against the surface-displayed ZnT8

Having established live-cell measurement of ZnT8-specific surface labeling, we interrogated human sera for immunofluorescence staining of live INS-1E cells. To eliminate serum autofluorescence and minimize serum-to-serum variation, we pooled eight ZnT8A-positive sera from patients with new-onset T1D (age/gender: 9.3/F, 6.3/F, 12.9/F, 13.1/M, 11.3/M, 15.4/M, 14.2/F, and 6.6/F) and five ZnT8A-negative sera from

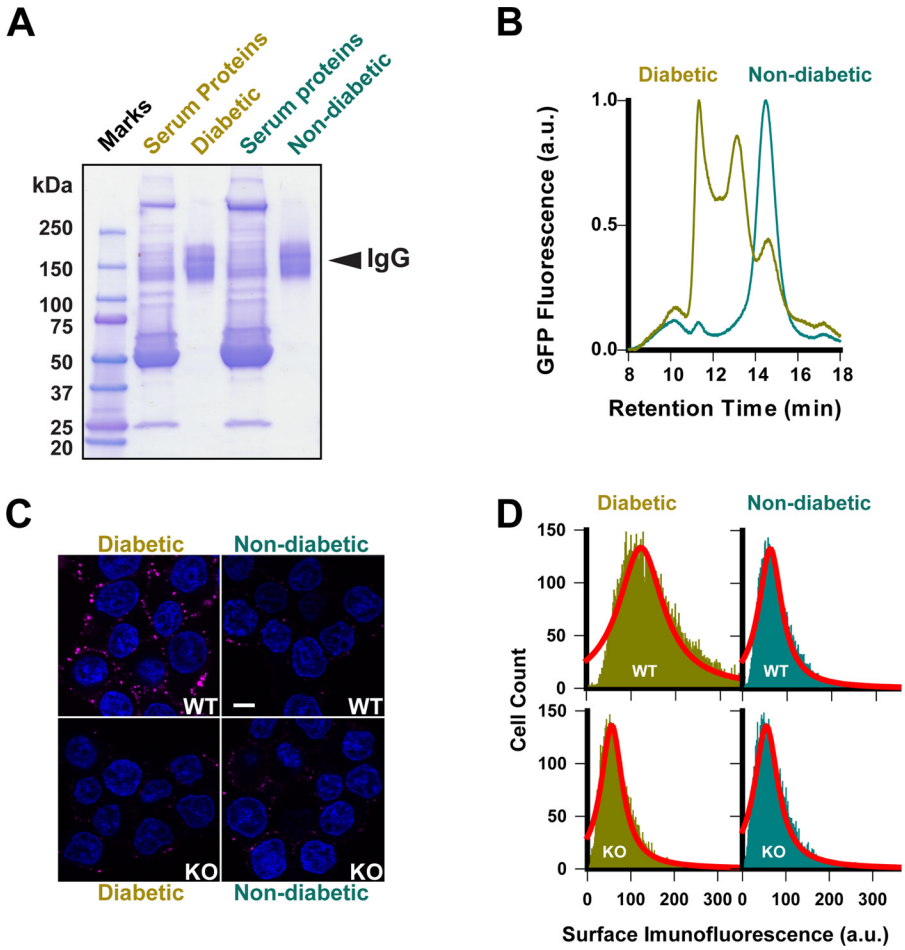

Figure 5. Anti-ZnT8 immunoreactivity of human sera. *A*, purification of whole IgG from human ZnT8A-positive and ZnT8A-negative sera. *B*, formation of ZnTA-ZnT8·GFP complexes as revealed by GFP fluorescence size exclusion HPLC of detergent-solubilized ZnT8·GFP exposed to purified IgG from diabetic patients as indicated. IgG from non-diabetic control subjects was analyzed in parallel as a negative control. *C*, representative confocal images of immunofluorescence staining of WT or ZnT8 KO cells using IgG from diabetic patients or non-diabetic control subjected as indicated. *Scale bar*, 20 μm. *D*, histograms of surface immunofluorescence intensities measured in >10,000 WT or *ZnT8* KO INS-1E cells that were stained by IgG from diabetic patients or non-diabetic control subjects as indicated. *Solid lines* are fits of histograms to a Lorentzian distribution.

non-diabetic control subjects (5.7/F, 16.6/M, 14.3/F, 16.9/M, and 14.3/F) and purified respective whole serum IgG by protein A/G affinity chromatography (Fig. 5*A*). Conformation-specific ZnT8A binding to detergent-solubilized ZnT8·GFP was evaluated by GFP size-exclusion HPLC, revealing three peaks using IgG from diabetic patients, corresponding to unbound ZnT8·GFP, 1:1 ZnT8A-ZnT8·GFP complex, and ZnT8A–cross-linked ZnT8·GFP multimers (Fig. 5*B*). In contrast, IgG from non-diabetic control subjects showed a single unbound ZnT8·GFP peak. Confocal microscopy imaging of live INS-1E cell staining revealed that IgG from diabetic patients produced a ring-like pattern of surface immunofluorescence, whereas control IgG only yielded some scattering signals (Fig. 5*C*). To evaluate ZnT8-specific immunofluorescence, we exposed KO cells to IgG from diabetic patients or non-diabetic control subjects under the identical experimental condition. The IgG from both sources stained KO cells at lower background levels (Fig. 5*C*). Average cell surface immunofluorescence was obtained by least squares fitting of flow cytometry histogram over 10,000 single cell recordings (Fig. 5*D*). Three independent experiments yielded highly reproducible results (Fig. S5), showing a marked 2.1-fold WT-KO difference in mean fluorescence intensity values for diabetic patients, in contrast to a small WT-KO difference for healthy control subjects. This result validated ZnT8-specific immunoreactivity directed to the surface of live pancreatic β-cells. The residual KO cell staining by IgG from both diabetic patients and non-diabetic control subjects was consistent with the heterogenous nature of islet cell surface antibodies in human sera (17).

Discussion

ZnT8 is ranked as one of the most transcriptionally enriched membrane proteins in the pancreatic β-cells (28). This zinc transporter is unique in its tissue-specific expression in pancreatic islets (29), mostly restricted to β-cells and to a lesser extent to non-β endocrine cells (30–32). We showed recently that glucose stimulation increases ZnT8 display on the surface of INS-1E cells (21). The secretion-coupled ZnT8 surfacing may enforce a vicious cycle of β-cell dysfunction and/or destruction during T1D progression (33). The ZnT8A assays reported herein uncovered a subclass of ZnT8A in human T1D sera that specifically recognized and reacted to ZnT8 on the surface of live pancreatic β-cells, leading to the identification of a molecular target of the elusive islet cell surface antibodies (18). This

finding is consistent with the detection of high levels of serum antibodies directed against homologous peptide epitopes derived from ZnT8 TMD and *Mycobacterium avium* subspecies paratuberculosis, a putative environmental agent triggering or accelerating T1D in Sardinian and Italian populations (34).

A marked difference in serum titers against ZnT8 and CTD suggested that ~50% proteoliposome-induced immunoreactivities were directed to epitopes in TMD. The anti-TMD immunoreactivity in mice correlates with humoral anti-TMD autoreactivity in humans (22). In 307 human serum samples, 17% of ZnT8A in sera from patients with T1D were attributed to anti-TMD only. Because this percentage did not include the incidence of polyclonal ZnT8As directed to both TMD and CTD, the estimated anti-TMD prevalence in sera of diabetic patients is lower than the estimated anti-TMD subpopulation in proteoliposome-immunized mouse sera (~50%). In the present study, purified antibodies from ZnT8A-positive sera of diabetic patients yielded a significantly higher surface immunofluorescence on WT INS-1E cells over a *ZnT8* KO background (Fig. 5). Validation of antibody specificity using KO-cells is a preferred method to establish a direct link between the gene, the target protein, and its detection by the antibody (35). Our experiments based on human–rat cross-reactivity and WT KO difference in surface immunofluorescence established ZnT8-specific humoral autoreactivity toward the surface-displayed ZnT8 in patients with T1D.

Growing evidence suggests that β-cell dysfunction is a primary defect in T1D pathogenesis together with the immune destruction of β-cells (36). Seroconversion to multiple islet autoantibodies is often triggered years before the symptoms of severe hyperglycemia (37), but the relationship between humoral autoreactivity and islet pathology remains unclear. The binding of ZnT8A to live pancreatic β-cells may allow a more direct pathogenic role for the surface-displayed ZnT8 in ZnT8A-mediated β-cell dysfunction and cytotoxicity without the killing of β-cells. In support of this notion, recent studies of autopsy specimens obtained from patients with T1D revealed quite modest immune cell infiltration (insulitis) in only 10–30% of total islets of affected human pancreas (38). This finding challenged the long-held belief that 80–90% of the β cell mass is lost at diagnosis (39). Future studies are needed to isolate monoclonal ZnT8As to elucidate their potential pathogenic roles in prediabetic and diabetic islets. The islet-specific expression of ZnT8, its accessibility to pharmacological modulations on the cell surface, and the prevalence as a major self-antigen in autoimmune diabetes may be translated to novel combinatorial therapies that target ZnT8 to correct β-cell dysfunction and promote immune protection at the same time.

Experimental procedures

Human sera

Experiments with human sera were reviewed and approved by Office of Human Subjects Research, Institutional Review Boards of Johns Hopkins University School of Medicine (IRB00124135).

ZnT8 KO mice

All experiments with mice were approved by the Institutional Animal Care and Use Committee of Johns Hopkins University School of Medicine. Full body, constitutive *Slc30a8* KO mice were obtained from Taconic Biosciences. Animal genotyping detected the deleted *Slc30a8* locus, and sequencing validation revealed a 19-nucleotide deletion in exon 2 with a frameshift mutation and a premature stop codon. Sequencing the G_1 generation ruled out predicted non-intergenic off-target mutations.

Antigen preparation

The human ZnT8 isoform-2 cDNA (NM_001172814.1) was subcloned into a mammalian pCMV6-based expression vector with a C-terminal His tag (26). The expression plasmid was introduced into FreeStyle 293-F cells by 293 fectin–mediated transfection and transiently expressed in suspension culture of a serum-free expression medium per manufacturer's instructions (Thermo Fisher Scientific). Human CTD-His was constructed by a N-terminal deletion to remove the entire TMD sequence from the ZnT8-His construct and transiently expressed in 293 cells as above. Cells expressing either ZnT8-His or CTD-His grew to a density of 1×10^6 cells/ml, were harvested 24 h post-transfection, and then were broken open using a microfluidizer. The membrane fraction was separated from the cytosolic fraction by ultracentrifugation. Purification of the membrane-bound ZnT8-His was described previously (26). The purified ZnT8-His was reconstituted at a ZnT8/lipid ratio of 1:20 (w/w) into proteoliposomes composed of DOPC, DOPE, and DOPG at a 2:1:1 ratio. Lipid A (Avanti catalog no. 699200P) was added as an adjuvant to the reconstitution lipid mixture to a concentration of 10% of the total lipid content. The reconstituted ZnT8-His in proteoliposomes was >95% pure, remained functionally active, and could be resolubilized by detergent to form a monodispersed species on sizing HPLC (26). Liposomes were prepared in parallel to proteoliposomes without adding ZnT8-His to the reconstitution lipid mixture. Human CTD-His in the cytosolic fraction of the cell lysate was purified by metal-chelating affinity chromatography.

Mouse immunization

Four pairs of male/female homozygous *Slc30a8*$^{-/-}$ mice at 7 weeks of age were used for proteoliposome immunization and a pair of male/female littermates for liposome immunization. Each mouse was first tail bled to collect non-immunized serum (M0) and then injected weakly with 60 μg of purified ZnT8 antigen in proteoliposome suspension or an equal volume of liposome suspension (200 μl) into the peritoneal cavity. Two weeks after the first injection, one mouse (M1) with proteoliposome immunization was euthanized to collect blood by cardiac puncture. The remaining nine mice (M2–M8 for proteoliposome immunization, and M9 and M10 for liposome immunization) were boosted with two additional weekly intraperitoneal injections and then euthanized 4 days after the last injection for terminal blood collection.

Enzyme-linked immunosorbent assay

For proteoliposome-based ELISA, 4 μg of proteoliposomes (containing 5% ZnT8-His by weight) diluted in 100 μl of PBS were added to each well of a high-binding 96-well plate (Thermo Fisher Scientific) and incubated overnight at 4 °C. The passively immobilized proteoliposomes were blocked with 5% BSA and then tested with sera in 3-fold serial dilutions. For solution-based ELISA, 0.6 μg of ZnT8-His from dodecyl-β-maltoside solubilized proteoliposomes or 0.3 μg of purified CTD-His in 100 μl of PBS were immobilized to each well of a nickel-coated 96-well plate via the C-terminal His tag. The immobilized protein was blocked by 5% BSA and then tested with sera in 3-fold serial dilutions. Bound serum antibodies were quantified by a HRP-conjugated goat anti-mouse IgG secondary antibody (Invitrogen, catalog no. 62-6520) with 1:3000 dilution on a Flexstation-3 microplate reader.

Immunoblotting

For assessment of serum anti-ZnT8 immunoreactivity, transfected or non-transfected FreeStyle 293-F cells (denoted as ZnT8(+) or ZnT8(−)) were used. SDS-solubilized cell lysate (10 μg) was subjected to SDS-PAGE and probed with a 1:1000 proteoliposome-immunized serum, 1:200 anti-ZnT8 (anti-TMD) rabbit pAb (Proteintech, catalog no. 16169-1-AP), or 1:1000 anti-ZnT8 (anti-CTD) mouse mAb (Amgen, Fig. S1), followed by 1:3000 anti-rabbit or anti-mouse HRP-conjugated secondary antibody (GE catalog no. NA934V or NA931V). For detection of ZnT8A-ZnT8·GFP protein complex, the HPLC peak fraction for the ZnT8A-ZnT8·GFP complex or ZnT8·GFP was collected (detailed below), concentrated by 10-fold using an Amicon MWCO 50-kDa centrifugal filter, and then subjected to SDS-PAGE. The resolved protein bands were probed using 1:2000 anti-GFP (Invitrogen, catalog no. PA5-22688) for ZnT8·GFP and 1:3000 sheep anti-mouse IgG (GE catalog no. NA931V) for mouse IgG.

INS-1E cells stably expressing ZnT8·GFP

Stably transfected INS-1E cells were selected by FACS based on cellular ZnT8·GFP fluorescence and grown as monolayers in complemented RMPI 1640 medium as described previously (19).

Fluorescence size-exclusion HPLC

Approximately 3×10^6 stably transfected INS-1E cells were solubilized using 200 μl of assay buffer (20 mM HEPES, 100 mM NaCl, pH 7.0) plus 0.5% dodecyl-β-maltoside. ZnT8·GFP in the detergent crude extract was collected as a monodispersed peak on GFP-fluorescence sizing-HPLC, incubated with 0.2 μl of proteoliposome- or liposome-immunized serum for 1 h, and then re-injected into the HPLC column. The elution profile was monitored using a fluorescence detector as described previously (19). The peak fractions were collected for immunoblotting analysis to validate the ZnT8A-ZnT8·GFP complex.

Immunofluorescence staining and imaging

For mouse sera, WT INS-1E cells grown on coverslips at ~70% confluence were exposed to a proteoliposome- or liposome-immunized serum at a 1:100 ratio in 100 μl of culture medium. After 2-h incubation in 37 °C, the cells were washed with Ca-PBS plus 1% BSA and then exposed to Alexa Fluor594 conjugated goat-anti-mouse secondary antibody in 1:200 dilution with culture medium (Thermo Fisher, catalog no. A11032). After 30 min of incubation at 4 °C, the cells were washed free of secondary antibody with Ca-PBS and then fixed with 4% paraformaldehyde. The nuclei were counterstained with DAPI. The cells were then imaged using a Zeiss LSM 700 inverted confocal microscope with a 100× oil objective under the control of Zen software (Zeiss). For human sera, 100 μg of purified whole IgG was used following the same procedure as above.

ZnT8 knock-out INS-1E cells

A custom sgRNA construct targeting exon 5 of *Slc30a8* and primers for performing SURVEYOR and sequencing analysis of the targeted locus were designed based on the online CRISPR Design Tool (28). A pair of 20-bp guide sequence oligonucleotides (CACAAAGGCCGCTCGAACGC) was annealed and ligated into a sgRNA expression plasmid pSpCas9(BB)-2A-GFP (PX458) (Addgene, ID 48138) containing a Cas9-GFP fusion. The sgRNA expression construct was validated by DNA sequencing and then delivered to low passage INS-1E cells (n = 33) by Lipofectamine 2000 transfection. The top 10% GFP-positive cells were FACS-sorted 48 h post-transfection. Genomic DNA from pooled GFP-positive cells was PCR amplified using the SURVEYOR primer pair (forward, ACGGTGAGCTCTATGCAAGC; and reverse, GTTTGAGCAAGTGAACGCGG). SURVEYOR nuclease digestion of reannealed amplicons suggested ~10% Cas9-mediated cleavage. Sorted cells were expanded clonally. Approximately 5×10^5 isogenic cells for each cell line were collected and screened by immunoblotting of SDS-lysate using 1:200 anti-ZnT8 pAb (Proteintech, catalog no. 16169-I-AP). Genomic DNAs from anti-ZnT8 negative cells were amplified with SURVEYOR primers, subcloned, and then sequenced to reveal the clonal genotype, showing a single nucleotide insert at the sgRNA cleavage site. This frameshift mutation abolished ZnT8 expression by anti-ZnT8 immunoblotting validation.

Flow cytometry analysis

WT or ZnT8 KO INS-1E cells were trypsinized, counted, and resuspended in the cell culture medium at a density of 1×10^6/ml. Aliquots of 100 μl of cell suspension were stained with 1 μl of a proteoliposome- or liposome-immunized mouse serum in 3-fold serial dilutions for 2 h at 37 °C, washed free of serum proteins with Hanks' balanced salt solution plus 1% BSA, and then stained with Alexa fluor647-conjugated donkey anti-mouse secondary antibody in 1:200 dilution with culture medium (Thermo Fisher, catalog no. A31571) for 30 min at 4 °C, followed by two washes with Hanks' balanced salt solution plus 1% BSA. The labeled cells were analyzed immediately by flow cytometry. Approximately 99% scattering events belonged to a singlet cell population with ~98% cell viability based on propidium iodide staining. The cells gated on forward and side scatter revealed a single population represented in a histogram of >10,000 single-cell counting events. The average immunofluorescence intensity and standard error were obtained by

least square fitting of the histogram to a Lorentzian distribution using the data analysis software SIGMAPLOT (SPSS Inc.). Parallel analyses were performed with human sera of diabetic patients or non-diabetic control subjects on 1×10^5 WT or ZnT8 KO INS-1E cells using 100 μg of purified whole serum IgG and 1 μg of Alexa Fluor 647-conjugated goat anti-human secondary antibody in 1:200 dilution (Thermo Fisher, catalog no. A21445).

Purification of human serum antibodies

Whole IgG from human sera were purified by affinity binding to immobilized protein-A/G on an agarose matrix per manufacturer's instructions (Pierce, catalog no. 20423).

Author contributions—C. M. and D. F. formal analysis; C. M., Q. H., and D. F. investigation; C. M., Q. H., and D. F. methodology; C. M., Q. H., W. G., and L. Y. writing-review and editing; Q. H. and D. F. data curation; W. G., L. Y., and D. F. resources; D. F. conceptualization; D. F. software; D. F. supervision; D. F. funding acquisition; D. F. validation; D. F. visualization; D. F. writing-original draft; D. F. project administration.

Acknowledgments—We thank Dr. Hao Zhang from the Flow Cytometry and Immunology Core Facility at Johns Hopkins Bloomberg School of Public Health for assistance in flow cytometry data acquisition and analysis. The Zeiss confocal microscope was supported through National Institutes of Health shared instrumentation Grant S10OD016374. The MoFlo XDP cell sorter was supported through National Institutes of Health Grants S10OD016315 and S10RR13777001.

References

1. Lemaire, K., Ravier, M. A., Schraenen, A., Creemers, J. W., Van de Plas, R., Granvik, M., Van Lommel, L., Waelkens, E., Chimienti, F., Rutter, G. A., Gilon, P., in't Veld, P. A., and Schuit, F. C. (2009) Insulin crystallization depends on zinc transporter ZnT8 expression, but is not required for normal glucose homeostasis in mice. *Proc. Natl. Acad. Sci. U.S.A.* **106,** 14872–14877 CrossRef Medline
2. Dang, M., Rockell, J., Wagner, R., Wenzlau, J. M., Yu, L., Hutton, J. C., Gottlieb, P. A., and Davidson, H. W. (2011) Human type 1 diabetes is associated with T cell autoimmunity to zinc transporter 8. *J. Immunol.* **186,** 6056–6063 CrossRef Medline
3. Chujo, D., Foucat, E., Nguyen, T. S., Chaussabel, D., Banchereau, J., and Ueno, H. (2013) ZnT8-specific CD4+ T cells display distinct cytokine expression profiles between type 1 diabetes patients and healthy adults. *PLoS One* **8,** e55595 CrossRef Medline
4. Énée, É., Kratzer, R., Arnoux, J. B., Barilleau, E., Hamel, Y., Marchi, C., Beltrand, J., Michaud, B., Chatenoud, L., Robert, J. J., and van Endert, P. (2012) ZnT8 is a major CD8+ T cell-recognized autoantigen in pediatric type 1 diabetes. *Diabetes* **61,** 1779–1784 CrossRef Medline
5. Li, S., Li, H., Chen, B., Lu, D., Deng, W., Jiang, Y., Zhou, Z., and Yang, Z. (2013) Identification of novel HLA-A 0201-restricted cytotoxic T lymphocyte epitopes from Zinc Transporter 8. *Vaccine* **31,** 1610–1615 CrossRef Medline
6. Scotto, M., Afonso, G., Larger, E., Raverdy, C., Lemonnier, F. A., Carel, J. C., Dubois-Laforgue, D., Baz, B., Levy, D., Gautier, J. F., Launay, O., Bruno, G., Boitard, C., Sechi, L. A., Hutton, J. C., *et al.* (2012) Zinc transporter (ZnT)8(186–194) is an immunodominant CD8+ T cell epitope in HLA-A2+ type 1 diabetic patients. *Diabetologia* **55,** 2026–2031 CrossRef Medline
7. Hinman, R. M., and Cambier, J. C. (2014) Role of B lymphocytes in the pathogenesis of type 1 diabetes. *Curr Diab Rep* **14,** 543 CrossRef Medline
8. Tooley, J. E., and Herold, K. C. (2014) Biomarkers in type 1 diabetes: application to the clinical trial setting. *Curr. Opin. Endocrinol. Diabetes Obes.* **21,** 287–292 CrossRef Medline
9. Palmer, J. P., Asplin, C. M., Clemons, P., Lyen, K., Tatpati, O., Raghu, P. K., and Paquette, T. L. (1983) Insulin antibodies in insulin-dependent diabetics before insulin treatment. *Science* **222,** 1337–1339 CrossRef Medline
10. Baekkeskov, S., Aanstoot, H. J., Christgau, S., Reetz, A., Solimena, M., Cascalho, M., Folli, F., Richter-Olesen, H., and Camilli, P. D. (1990) Identification of the 64K autoantigen in insulin-dependent diabetes as the GABA-synthesizing enzyme glutamic acid decarboxylase. *Nature* **347,** 151–156 CrossRef Medline
11. Rabin, D. U., Pleasic, S. M., Shapiro, J. A., Yoo-Warren, H., Oles, J., Hicks, J. M., Goldstein, D. E., and Rae, P. M. (1994) Islet cell antigen 512 is a diabetes-specific islet autoantigen related to protein tyrosine phosphatases. *J. Immunol.* **152,** 3183–3188 Medline
12. Wenzlau, J. M., Juhl, K., Yu, L., Moua, O., Sarkar, S. A., Gottlieb, P., Rewers, M., Eisenbarth, G. S., Jensen, J., Davidson, H. W., and Hutton, J. C. (2007) The cation efflux transporter ZnT8 (Slc30A8) is a major autoantigen in human type 1 diabetes. *Proc. Natl. Acad. Sci. U.S.A.* **104,** 17040–17045 CrossRef Medline
13. Wenzlau, J. M., and Hutton, J. C. (2013) Novel diabetes autoantibodies and prediction of type 1 diabetes. *Curr Diab Rep* **13,** 608–615 CrossRef Medline
14. Wenzlau, J. M., Moua, O., Sarkar, S. A., Yu, L., Rewers, M., Eisenbarth, G. S., Davidson, H. W., and Hutton, J. C. (2008) SlC30A8 is a major target of humoral autoimmunity in type 1 diabetes and a predictive marker in prediabetes. *Ann. N.Y. Acad. Sci.* **1150,** 256–259 CrossRef Medline
15. Yu, L., Boulware, D. C., Beam, C. A., Hutton, J. C., Wenzlau, J. M., Greenbaum, C. J., Bingley, P. J., Krischer, J. P., Sosenko, J. M., Skyler, J. S., Eisenbarth, G. S., Mahon, J. L., and Type 1 Diabetes TrialNet Study Group (2012) Zinc transporter-8 autoantibodies improve prediction of type 1 diabetes in relatives positive for the standard biochemical autoantibodies. *Diabetes Care* **35,** 1213–1218 CrossRef Medline
16. Lernmark, A., Freedman, Z. R., Hofmann, C., Rubenstein, A. H., Steiner, D. F., Jackson, R. L., Winter, R. J., and Traisman, H. S. (1978) Islet-cell-surface antibodies in juvenile diabetes mellitus. *N. Engl. J. Med.* **299,** 375–380 CrossRef Medline
17. Van De Winkel, M., Smets, G., Gepts, W., and Pipeleers, D. (1982) Islet cell surface antibodies from insulin-dependent diabetics bind specifically to pancreatic B cells. *J. Clin. Invest.* **70,** 41–49 CrossRef Medline
18. Dobersen, M. J., and Scharff, J. E. (1982) Preferential lysis of pancreatic B-cells by islet cell surface antibodies. *Diabetes* **31,** 459–462 CrossRef Medline
19. Peterson, C., Campbell, I. L., and Harrison, L. C. (1992) Lack of specificity of islet cell surface antibodies (ICSA) in IDDM. *Diabetes Res. Clin. Pract.* **17,** 33–42 CrossRef Medline
20. Vives, M., Somoza, N., Soldevila, G., Gomis, R., Lucas, A., Sanmarti, A., and Pujol-Borrell, R. (1992) Reevaluation of autoantibodies to islet cell membrane in IDDM. Failure to detect islet cell surface antibodies using human islet cells as substrate. *Diabetes* **41,** 1624–1631 CrossRef Medline
21. Huang, Q., Merriman, C., Zhang, H., and Fu, D. (2017) Coupling of insulin secretion and display of a granule-resident zinc transporter ZnT8 on the surface of pancreatic β cells. *J. Biol. Chem.* **292,** 4034–4043 CrossRef Medline
22. Wan, H., Merriman, C., Atkinson, M. A., Wasserfall, C. H., McGrail, K. M., Liang, Y., Fu, D., and Dai, H. (2017) Proteoliposome-based full-length ZnT8 self-antigen for type 1 diabetes diagnosis on a plasmonic platform. *Proc. Natl. Acad. Sci. U.S.A.* **114,** 10196–10201 CrossRef Medline
23. Merriman, C., Huang, Q., Rutter, G. A., and Fu, D. (2016) Lipid-tuned zinc transport activity of human ZnT8 protein correlates with risk for type-2 diabetes. *J. Biol. Chem.* **291,** 26950–26957 CrossRef Medline
24. Merglen, A., Theander, S., Rubi, B., Chaffard, G., Wollheim, C. B., and Maechler, P. (2004) Glucose sensitivity and metabolism-secretion coupling studied during two-year continuous culture in INS-1E insulinoma cells. *Endocrinology* **145,** 667–678 CrossRef Medline
25. Declerck, P. J., Carmeliet, P., Verstreken, M., De Cock, F., and Collen, D. (1995) Generation of monoclonal antibodies against autologous proteins

in gene-inactivated mice. *J. Biol. Chem.* **270,** 8397–8400 CrossRef Medline
26. Davidson, H. W., Wenzlau, J. M., and O'Brien, R. M. (2014) Zinc transporter 8 (ZnT8) and β cell function. *Trends Endocrinol. Metab.* **25,** 415–424 CrossRef Medline
27. Cong, L., Ran, F. A., Cox, D., Lin, S., Barretto, R., Habib, N., Hsu, P. D., Wu, X., Jiang, W., Marraffini, L. A., and Zhang, F. (2013) Multiplex genome engineering using CRISPR/Cas systems. *Science* **339,** 819–823 CrossRef Medline
28. Segerstolpe, Å., Palasantza, A., Eliasson, P., Andersson, E. M., Andréasson, A. C., Sun, X., Picelli, S., Sabirsh, A., Clausen, M., Bjursell, M. K., Smith, D. M., Kasper, M., Ämmälä, C., and Sandberg, R. (2016) Single-cell transcriptome profiling of human pancreatic islets in health and type 2 diabetes. *Cell Metab* **24,** 593–607 CrossRef Medline
29. Lemaire, K., Chimienti, F., and Schuit, F. (2012) Zinc transporters and their role in the pancreatic β-cell. *J Diabetes Investig* **3,** 202–211 CrossRef Medline
30. Gyulkhandanyan, A. V., Lu, H., Lee, S. C., Bhattacharjee, A., Wijesekara, N., Fox, J. E., MacDonald, P. E., Chimienti, F., Dai, F. F., and Wheeler, M. B. (2008) Investigation of transport mechanisms and regulation of intracellular Zn^{2+} in pancreatic α-cells. *J. Biol. Chem.* **283,** 10184–10197 CrossRef Medline
31. Tamaki, M., Fujitani, Y., Uchida, T., Hirose, T., Kawamori, R., and Watada, H. (2009) Downregulation of ZnT8 expression in pancreatic β-cells of diabetic mice. *Islets* **1,** 124–128 CrossRef Medline
32. Murgia, C., Devirgiliis, C., Mancini, E., Donadel, G., Zalewski, P., and Perozzi, G. (2009) Diabetes-linked zinc transporter ZnT8 is a homodimeric protein expressed by distinct rodent endocrine cell types in the pancreas and other glands. *Nutr. Metab. Cardiovasc. Dis.* **19,** 431–439 CrossRef Medline
33. Atkinson, M. A., Bluestone, J. A., Eisenbarth, G. S., Hebrok, M., Herold, K. C., Accili, D., Pietropaolo, M., Arvan, P. R., Von Herrath, M., Markel, D. S., and Rhodes, C. J. (2011) How does type 1 diabetes develop?: the notion of homicide or β-cell suicide revisited. *Diabetes* **60,** 1370–1379 CrossRef Medline
34. Niegowska, M., Rapini, N., Piccinini, S., Mameli, G., Caggiu, E., Manca Bitti, M. L., and Sechi, L. A. (2016) Type 1 diabetes at-risk children highly recognize *Mycobacterium avium* subspecies paratuberculosis epitopes homologous to human Znt8 and Proinsulin. *Sci Rep* **6,** 22266 CrossRef Medline
35. Uhlen, M., Bandrowski, A., Carr, S., Edwards, A., Ellenberg, J., Lundberg, E., Rimm, D. L., Rodriguez, H., Hiltke, T., Snyder, M., and Yamamoto, T. (2016) A proposal for validation of antibodies. *Nat. Methods* **13,** 823–827 Medline
36. Tersey, S. A., Nishiki, Y., Templin, A. T., Cabrera, S. M., Stull, N. D., Colvin, S. C., Evans-Molina, C., Rickus, J. L., Maier, B., and Mirmira, R. G. (2012) Islet β-cell endoplasmic reticulum stress precedes the onset of type 1 diabetes in the nonobese diabetic mouse model. *Diabetes* **61,** 818–827 CrossRef Medline
37. Ziegler, A. G., Rewers, M., Simell, O., Simell, T., Lempainen, J., Steck, A., Winkler, C., Ilonen, J., Veijola, R., Knip, M., Bonifacio, E., and Eisenbarth, G. S. (2013) Seroconversion to multiple islet autoantibodies and risk of progression to diabetes in children. *JAMA* **309,** 2473–2479 CrossRef Medline
38. Campbell-Thompson, M., Fu, A., Kaddis, J. S., Wasserfall, C., Schatz, D. A., Pugliese, A., and Atkinson, M. A. (2016) Insulitis and β-cell mass in the natural history of type 1 diabetes. *Diabetes* **65,** 719–731 CrossRef Medline
39. von Herrath, M., Sanda, S., and Herold, K. (2007) Type 1 diabetes as a relapsing-remitting disease? *Nat. Rev. Immunol.* **7,** 988–994 CrossRef Medline